



Contents lists available at ScienceDirect

International Journal for Parasitology

journal homepage: www.elsevier.com/locate/ijpara

Continuous culture of *Cryptosporidium parvum* using hollow fiber technology

Mary Morada^a, Sangun Lee^b, Leslie Gunther-Cummins^c, Louis M. Weiss^{d,e}, Giovanni Widmer^b, Saul Tzipori^b, Nigel Yarlett^{a,*}

^aHaskins Laboratories, and Department of Chemistry and Physical Sciences, Pace University, New York, USA

^bCummings School of Veterinary Medicine, Tufts University, N. Grafton, MA, USA

^cAnalytical Imaging Facility, Albert Einstein College of Medicine, Bronx, NY, USA

^dDepartment of Pathology, Albert Einstein College of Medicine, Bronx, NY, USA

^eDepartment of Medicine, Albert Einstein College of Medicine, Bronx, NY, USA

ARTICLE INFO

Article history:

Received 21 January 2015

Received in revised form 23 July 2015

Accepted 24 July 2015

Available online xxxxx

Keywords:

Cryptosporidium

In vitro culture

Hollow-fiber

Anaerobic

ABSTRACT

Diarrheal disease is a leading cause of pediatric death in economically low resource countries. *Cryptosporidium* spp. are the second largest member of this group and the only member for which no treatment exists. One of the handicaps to developing chemotherapy is the lack of a reproducible long-term culture method permitting in vitro drug screening beyond 48 h. We have adapted the well-established hollow fiber technology to provide an environment that mimics the gut by delivering nutrients and oxygen from the basal layer upwards while allowing separate redox and nutrient control of the lumen for parasite development. Using this technique, oocyst production was maintained for >6 months, producing approximately 1×10^8 oocysts $\text{ml}^{-1} \text{day}^{-1}$, compared with 48 h with a yield of 1×10^6 oocysts ml^{-1} in two-dimensional cultures. Oocysts, after 4 and 20 weeks in culture, produced a chronic infection in a TCR- α -deficient mouse model. In vivo infectivity of oocysts was confirmed using oocysts from a 6 week culture in a dexamethasone immunosuppressed mouse model.

© 2015 Australian Society for Parasitology Inc. Published by Elsevier Ltd. All rights reserved.

1. Introduction

Cryptosporidium spp. are the second (after rotavirus) leading cause of diarrheal disease and death in infants in economically low resource countries (Liu et al., 2012), and remains the only member of the major diarrheal diseases for which no consistently effective therapy is available. In parts of Asia and Africa as many as 31.5% of all children under 2 years of age are infected with the parasite, posing a significant health risk (Kotloff et al., 2013; Checkley et al., 2014). There are five species responsible for infections in humans, *Cryptosporidium hominis*, *Cryptosporidium parvum*, *Cryptosporidium meleagridis*, *Cryptosporidium canis* and *Cryptosporidium felis*, of which *C. hominis* or *C. parvum* are the most common (Xiao, 2010). Infection of the epithelial cells of the gastrointestinal tract by this parasite results in an acute watery diarrhea, which can become life threatening in children, the elderly and immune-compromised individuals (Mathur et al., 2013). Malnourished chil-

dren are at a greater risk of death from the infection and those that survive are at greater risk of stunted growth and wasting (Banwat et al., 2003; Hamed et al., 2005; Checkley et al., 2014). The underlying cause of disease transmission is poor hygiene and contaminated water sources (Molloy et al., 2011; Mølbak et al., 2013). In some countries it is endemic due to the poor sanitation and lack of appropriate health practices. Despite the significant morbidity and mortality associated with cryptosporidiosis, drug discovery lags behind that of many other infectious diseases (Striepen, 2013). Nitazoxanide, the only FDA-approved drug for treatment of cryptosporidiosis, is not effective in immune-compromised individuals and is not routinely used in standard care in countries such as India (Abubakar et al., 2007).

The parasite has a multistage life cycle producing thick walled oocysts that are shed from infected individuals and act as the infective stage; other stages include motile sporozoites, merozoites, macro- and microgametes, as well as thin-walled oocysts that are responsible for autoinfection. In common with other members of the Apicomplexa, *Cryptosporidium* spp. require a host cell to complete the life cycle. The parasite is capable of parasitising a number of in vitro cultured cell lines (Upton et al., 1994) producing thin walled oocysts that are not infective to the primary host.

* Corresponding author at: Haskins Laboratories, and Department of Chemistry and Physical Sciences, Pace University, 41 Park Row, New York, NY 10038, USA. Tel.: +1 212 346 1853; fax: +1 212 346 1586.

E-mail address: nyarlett@pace.edu (N. Yarlett).

Significant advances have been reported, (reviewed by Arrowood (2008)). More recent is the use of an HCT-8 organoid model to replicate the intestine (Alcantara Warren et al., 2008), and the use of primary cultured intestinal epithelial cells (Castellanos-Gonzalez et al., 2013) which have extended the in vitro infection to >5 days. Recently Varughese et al. (2014) described a model using small intestinal epithelial cells, FHs 74 Int, demonstrating improved infection kinetics that has great potential for host-parasite studies. It was the goal of this study to extend the in vitro culture of *C. parvum* to >1 month, permitting long-term drug studies to be performed. We considered the following issues as critical to the development of a long-term culture system. The presence of two controlled environments (biphasic) would provide host cells with oxygen and nutrients from the basal layer, while allowing a low oxygen nutrient rich environment to be developed on the apical surface where the parasite would be present, thus mimicking the situation in situ. The development of such a system provides the added advantage of allowing the development of a parasite-specific growth medium, which is not possible in current two-dimensional (2D) cultures where emphasis is directed to maintaining host cell growth to support the parasite burden. The parasite completes its life cycle within the host intestine, a low oxygen environment. In addition, a microaerophilic parasite metabolism is inferred from genome sequence information (Abrahamsen et al., 2004), and is supported by several studies demonstrating the loss of typical mitochondria (Hieinz and Lithgow, 2013), and dependence upon a low oxygen metabolism, reviewed by Zhu (2008). These observations prompted us to modify the standard medium developed by Upton et al. (1994) to include reducing agents and a mixture of fatty acids, which have been shown to be important in the growth of various anaerobic protozoa (Yichoy et al., 2011).

2. Materials and methods

2.1. Culture of HCT-8 host cells

Human ileocecal colorectal adenocarcinoma cells (HCT-8 (HRT-18), ATCC CCL-244) were used to provide a host cell layer on the extra-capillary surface of the fibers. MEM plus supplements and serum (MEMSS) (Upton et al., 1994) circulated through the hollow fibers and glucose levels were recorded using an Accu-Chek Active monitor (Hoffmann-La Roche Ltd., Indianapolis, IN, USA). The pH was monitored by sampling 5 mL of the recirculating medium using a Corning 440 pH meter (Corning, NY, USA).

2.2. Real-time quantitative reverse transcription-PCR (qRT-PCR) analysis of parasite 18S rRNA

Total RNA was isolated from 5 ml of *C. parvum* and host cells collected from the cartridge. The sample was centrifuged at 6449g for 5 min in a swing-out rotor (Beckman-Coulter, Indianapolis, IN, USA), then the pellet was resuspended in 200 μ l of PBS and washed three times; 50 μ l was removed and the remainder centrifuged, resuspended in lysis buffer (iScript RT-qPCR sample preparation reagent, Bio-Rad Laboratories, Hercules, CA, USA) and subjected to six cycles of freezing-thawing using liquid nitrogen and a 65 °C heating block. Total RNA was isolated using RNeasy (Qiagen Inc., Valencia, CA, USA) and the total RNA was determined using a Qubit 3.0 fluorometer (Life Technologies, Thermo-Fisher Scientific Inc., Waltham, MA, USA). RNA was adjusted to 5 ng/ μ l and the parasite, *C. parvum* (Cp)18S rRNA, and human, (h)18S rRNA, detected using the primers described by Cai et al. (2005), Cp18S-995F: 5'-TAGAGATTGGAGTTCCT-3' and Cp18S-1206R: 5'-CTCCACCAACTAAGAACGCC-3'; the primers for human 18S-RNA were

Hs18S-F1373: 5'-CCGATAACGAACGAGACTCTGG-3', and Hs18S-R1561: 5'-TAGGGTAGGCACACGCTGAGCC-3'. The expected sizes of the parasite and human amplicons obtained were 212 bp and 189 bp, respectively. Cp18S rRNA and h18S rRNA was quantitated by qRT-PCR using an iScript One-Step qRT-PCR kit with SYBR green (Bio-Rad Laboratories). Total RNA (5 ng), reagents and primers were incubated at 48 °C for 30 min, followed by 95 °C for 10 min, and then subjected to 40 thermal cycles of 95 °C for 15 s and 60 °C for 1 min. A melting curve was performed by heating to 95 °C for 15 s, followed by 60 °C for 15 s and 95 °C for 15 s, using a QuantStudio 6 Flex Real-Time PCR System (Life Technologies, Thermo-Fisher Scientific Inc., Waltham, MA, USA). The qRT-PCR analysis was also performed for the Iowa isolate (Bunch Grass Farms, Deary, ID, USA), diluted to give 10⁵, 10⁶ and 10⁷ oocysts. The ΔC_T for parasite 18S rRNA was determined by subtraction of the C_T for h18S rRNA from the C_T for parasite Cp18S rRNA.

2.3. Immunocompromised and immunosuppressed mouse models

Oocysts collected from the culture system were tested for the ability to infect two well established mouse models. Oocysts were collected at specified times from the culture system, stored in 2.5% potassium dichromate at 4 °C for less than 1 month, washed with distilled water three times to remove the potassium dichromate, and enumerated using a hemacytometer prior to use.

The first model employed nine 6 week old female TCR- α -deficient mice on a C57BL/6 background (Jackson Laboratories, Bar Harbor, ME, USA); mice were segregated into groups of three; three were infected per os with 10⁴ oocysts in 200 μ l of PBS collected after 4 and 20 weeks in culture; three were infected with 10⁴ oocysts of the Iowa isolate used to establish the culture; three were administered 200 μ l of PBS as negative controls. All mice were housed in metabolic chambers (VWR, Atlanta, GA, USA) and every 24 h feces were removed, weighed and placed into potassium dichromate for storage. After 7 days, mice were euthanised by CO₂ asphyxiation as recommended by the American Veterinary Medical Association (AVMA) (Pace University, NY, USA) and intestinal sections from the distal ileum-cecum and proximal colon removed and fixed in 10% neutral buffered formalin (3.7–4.0% formaldehyde in 33.3 mM monosodium phosphate and 45.8 mM disodium phosphate buffer).

The second model employed 15 female CD-1[®] IGS mice (Charles River Laboratory, Wilmington, MA, USA) aged 3–5 weeks, weighing 17–22 g each, which were immunosuppressed with dexamethasone 21-phosphate (D1159, Sigma, USA) administered ad libitum in drinking water (16 μ g/ml) from 4 days prior to inoculation to the end of the study. Mice were separated into the following three groups of five per group, and infected per os with 200 μ l of sterile water containing either 10⁶ oocysts from 6 weeks in culture (group 1), the parent Iowa isolate used to initiate the culture (group 2) or were an uninfected control group (group 3). Mice were monitored twice daily following the infection and weighed three times per week; fecal samples were collected daily for 17 days and fecal smears stained using the modified Kinyoun acid fast method (Ma and Soave, 1983). After 17 days, mice were euthanised by CO₂ asphyxiation as recommended in the AVMA (Tufts University, MA, USA) and gastrointestinal sections removed for histopathological examination. The ileum, cecum and proximal colon were fixed in 10% natural buffered formalin and processed for H&E stains.

Animal studies were performed in strict accordance with the recommendations in the Guide for the Care and Use of Laboratory Animals of the National Institutes of Health, USA under the Animal Welfare Assurance numbers A3112-01 (Pace University, Haskins Laboratories, NYC, USA) and A4059-01 (Tufts University, Cummings School of Veterinary Medicine, USA). Animal experiments were performed in accordance with the procedures approved by

the Institutional Animal Care and Use Committees of Pace University, NYC and Tufts University, Cummings School Veterinary Medicine, MA, USA.

2.4. Staining with fluorescently labeled antibodies

Samples (5–10 mL) were removed from the extra capillary space of the cartridge by displacement using two 10 mL sterile syringes. Samples were centrifuged at 16,162g for 1 min (Sorvall Biofuge Fresco, Thermo Fisher Scientific) and the pellet resuspended in Dulbecco's PBS. Oocysts were stained using 50 μ L of FITC-labeled mouse monoclonal antibody to *C. parvum* oocyst surface proteins (Crypt-a-Glo[®], Waterborne Inc., New Orleans, LA, USA) and incubated in the dark at room temperature for 30 min, after which time they were washed twice with PBS and examined using a fluorescence microscope (Nikon Optiphot, Melville, NY, USA) with an excitation λ 410–485 nm, and an emission λ 515 nm. Samples were counter-stained with a fluorescent-labeled polyclonal antibody specific for sporozoites and other motile intracellular stages (Sporo-Glo[®], Waterborne Inc.), and examined using an excitation λ 535–550 nm, and an emission λ 580 nm.

2.5. Preparation of oocysts and excystation

Cryptosporidium parvum oocysts were purified from the other stages (empty oocyst shells, host cells, etc) using isopycnic percoll gradient centrifugation (Arrowood and Sterling, 1987) consisting of 3 mL of 1.04 g mL⁻¹ percoll overlaid onto 5 mL of 1.08 g mL⁻¹ percoll. One millilitre samples from the cartridge were layered onto these gradients and centrifuged at 400g for 30 min. The oocysts formed a light colored band approximately 1/3 of the distance from the bottom of the tube and were then aspirated and washed with PBS by centrifugation at 1000g for 10 min. Sporozoites were obtained by excysting oocysts in MEM containing 0.25% trypsin, 0.75% taurodeoxycholate at 37 °C in a shaking water bath.

2.6. Polyamine analysis

Polyamines were separated and identified by reverse phase HPLC using a Perkin Elmer LC410 system coupled to a C18 10 μ m column (4.5 \times 250 mm) at a flow rate of 1 mL min⁻¹. The method employed a 40 min discontinuous gradient starting with 90% (v/v) buffer A (0.1 M NaH₂PO₄, 8 mM octanesulfonic acid, and 0.05 mM EDTA) and 10% (v/v) buffer B (acetonitrile). The initial conditions were held for 5 min before changing to 20% buffer B for 15 min, 40% buffer B for a further 10 min, and then returning to 10% buffer B for 10 min (Morada et al., 2013). Samples and standards were mixed 1:1 with 1.5 mM *o*-phthalaldehyde (dissolved in 0.5 M boric acid, 0.43 M KOH and 0.014 M β -mercaptoethanol) using a post column pump and detected using a Perkin Elmer fluorescence detector (excitation wavelength 320 nm, emission wavelength 455 nm). Areas under the peaks were determined using β -RAM computer software (IN/US Systems). Results were obtained using three separate oocyst preparations obtained from the cartridge.

2.7. Enzyme assays

Spermidine/spermine *N*¹-acetyltransferase (SSAT) was determined using 100 μ M bicine buffer (pH 8.0) containing 17 μ M [1-¹⁴C]acetyl-CoA (60 μ Ci/mmol) and supplemented with 50 μ M unlabeled acetyl-CoA, 500 μ M spermine and 25 μ g of protein. The reaction was stopped after 30 min with ice-cold 50 mM hydroxylamine, placed in a boiling water bath for 3 min, cooled and centrifuged at 9000g for 1 min to remove precipitated protein.

The supernatant (50 μ L) was spotted onto filter discs, dried and washed with 6 \times 200 mL changes of distilled water to remove unreacted [1-¹⁴C]-acetyl-CoA, with a final wash with 200 mL of methanol. The dried discs were placed in 10 mL of Omni Fluor and the radioactivity present as [¹⁴C]-acetylspermine was counted using a Beckman Tri-Carb 1600CA liquid scintillation counter (Perkin Elmer Life Sciences, Waltham, MA, USA). Blanks containing [1-¹⁴C] acetyl-CoA and spermine without protein were also analyzed and subtracted from the experimental results (Morada et al., 2013).

Spermidine acetyl transferase (SAT) was assayed using the same method for SSAT but using 500 μ M spermidine in place of spermine (Keithly et al., 1997).

S-adenosyl-L-methionine decarboxylase (putrescine stimulated) was determined by measuring the ¹⁴CO₂ produced from 0.5 μ Ci [1-¹⁴C-carboxyl]-S-adenosylmethionine (55 mCi/mmol) incubations containing 10 mM Tris-HCl pH 6.5 and 1 mM putrescine (Keithly et al., 1997). The ¹⁴CO₂ released in 60 min was trapped on benzethonium hydroxide soaked filter paper and counted by scintillation using a Beckman Tri-Carb 1600CA liquid scintillation counter (Perkin Elmer Life Sciences).

2.8. Electron microscopy

For Scanning Electron Microscopy (SEM), samples were fixed in 2.5% glutaraldehyde, 0.1 M sodium cacodylate pH 7.4, dehydrated through a graded series of ethanol, critical point dried using liquid carbon dioxide in a Tousimis Samdri 790 Critical Point Drier (Rockville, MD, USA) and sputter coated with gold-palladium in a Denton Vacuum Desk-2 Sputter Coater (Cherry Hill, NJ, USA). The samples were examined in a JEOL JSM6400 Scanning Electron Microscope (Peabody, MA, USA), using an accelerating voltage of 10 kV. Images were recorded with AnalySIS, Soft Imaging Systems (Munster, Germany).

2.9. Statistics

The statistical comparison of the differences among experimental groups was made by Mann-Whitney *U* test using GraphPad Prism 5 software (GraphPad Software, San Diego, CA, USA). Results were considered to be statistically significant at *P* < 0.05.

3. Results

We describe a method for the long-term in vitro culture of *C. parvum* in a simulated gut-like environment using hollow fiber technology. Human ileocecal adenocarcinoma (HCT-8; ATCC CCL 244) cells were selected as the cell line to support growth of *C. parvum* because previous studies found this cell line supported a greater infection than alternative ones (Upton et al., 1994; Meloni and Thompson, 1996), a feature that does not diminish with age of the cells (Sifuentes and DiGiovanni, 2007). HCT-8 cells have also been shown to differentiate into organoids that express normal intestinal tissue markers, and morphologically produce microvilli and desmosomes characteristic of normal intestinal tissue (Carvalho et al., 2005). We considered these features ideal for a long-term in vitro culture system. A 20 ml hollow fiber cartridge (CS2011; FiberCell[®] Systems, Inc., Frederick, MD, USA), conditioned according to the manufacturer's instructions, was inoculated with 10⁸ HCT-8 cells via the side port, and a 125 mL reservoir containing MEMSS (Upton et al., 1994) circulated through the hollow fibers at a flow rate of 51 mL min⁻¹ (setting five; Fig. 1). The fiber surface area (2100 cm²) provides efficient nutrient, metabolite and gas exchange between the HCT-8 cell layer and the re-circulating medium. The cartridge, pump and growth medium were kept inside a

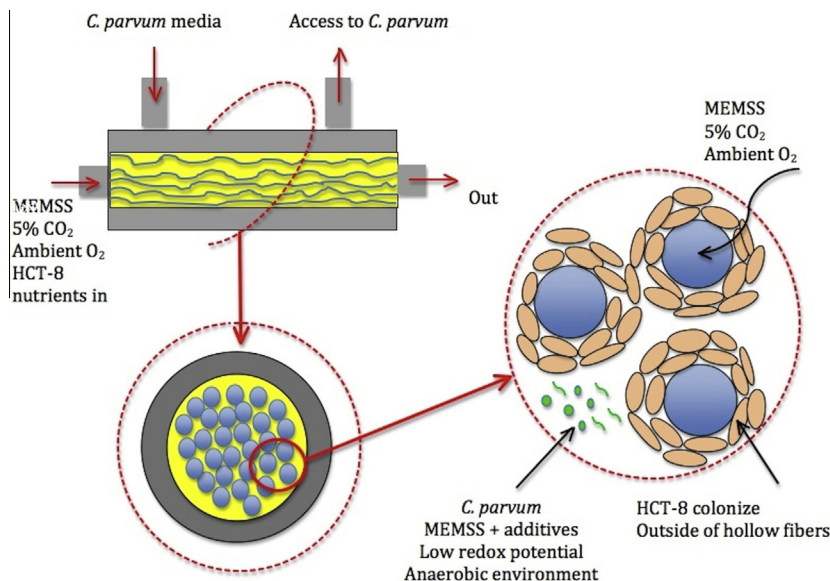


Fig. 1. Diagram of the hollow fiber system. The cartridge is composed of 200 μm diameter polysulfone hollow fibers with a 20 kDa molecular weight cut-off. The growth medium (MEM plus supplements and serum, MEMSS) was pumped through the fibers to supply nutrients and oxygen to, and remove waste products from, the host cells (HCT-8) which colonize the outside of the hollow fibers. The extra capillary space was inoculated with *Cryptosporidium parvum* and the MEMSS medium in this environment was modified to include additives that promote parasite growth - lipids, redox buffers and vitamins (as described in Section 3). Additions can be made and parasites removed from the extra capillary space using the side port shown on the top of the cartridge.

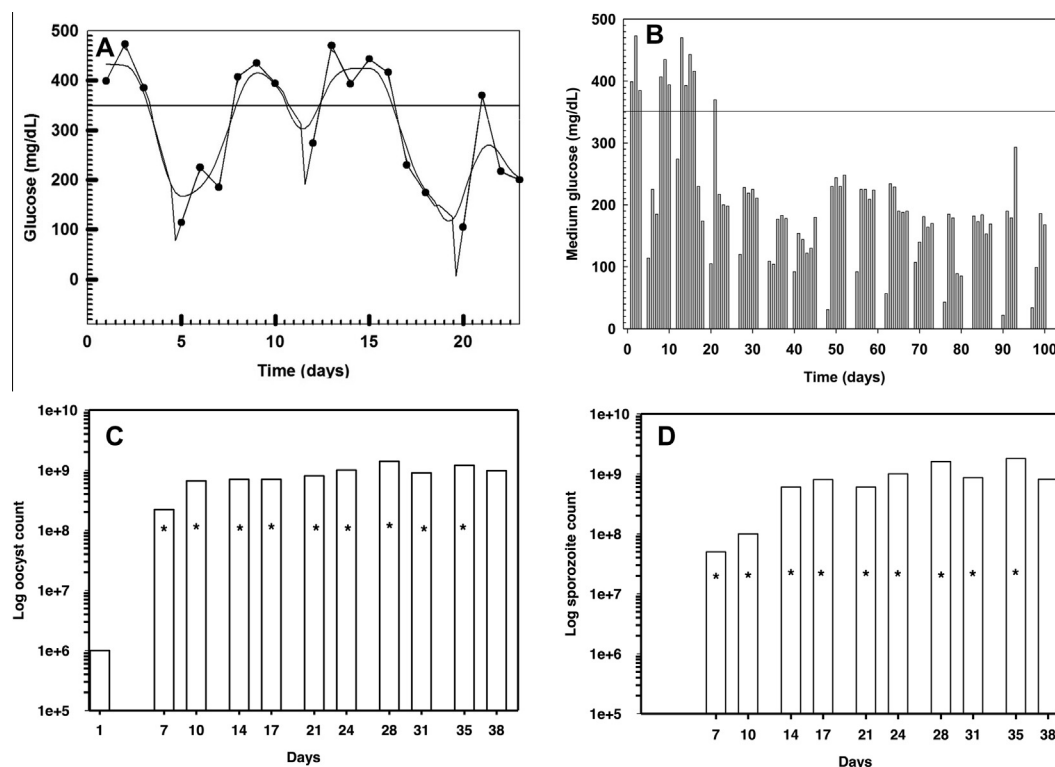


Fig. 2. Daily glucose and cell counts from the hollow fiber culture system. (A) The cartridge was inoculated with 10^8 HCT-8 cells and allowed to achieve confluence for 11 days. On day 12 the cartridge was inoculated with 10^6 *Cryptosporidium parvum* oocysts and the glucose levels monitored daily. Twenty-four hours p.i. there was an initial increase in medium glucose levels associated with infection of host cells by *C. parvum*. The increase in glucose levels may be due to disruption of the host cell monolayer, resulting in lysis and release of stored glycogen. (B) The pattern of medium glucose levels (bars) cycled for approximately 20 days and exhibited a dampened oscillation, indicative of loss of synchrony of the parasitemia of host cells by *C. parvum*. The line at 350 mg dL^{-1} is the glucose concentration of the MEM plus supplements and serum (MEMSS) growth media circulated through the microfibers. (C) Seven days p.i., half of the extra capillary volume (7.5 mL) was removed for enumeration of oocysts and sporozoites. This was repeated at 3–4 day intervals; asterisks indicate removal of 50% of the extra capillary volume and replacement with fresh medium. Oocysts were stained with a fluorescent-labeled mouse anti-*C. parvum* oocyst wall monoclonal antibody and counted using a hemacytometer by fluorescence microscopy with an excitation λ 410 nm–485 nm and an emission λ of 515 nm. (D) Sporozoites were counted using a hemacytometer after staining with a polyclonal antibody to intracellular and motile stages (Sporo-Glo[®], Waterborne Inc., New Orleans, LA, USA) using an excitation λ 535 nm–550 nm and an emission wavelength of 580 nm.

5% CO₂ incubator maintained at 37 °C. At 24 h intervals the glucose (Fig. 2A) and pH levels (data not shown) were recorded. When the glucose fell below 50% of the fresh MEMSS, the reservoir volume was doubled to 250 ml, and this process was continued until a reservoir volume of 1 L was achieved (8–11 days); when the HCT-8 cells were at full confluent density the pump rate was increased to 105 ml min⁻¹ (setting 10).

3.1. Redox and nutrient requirements

The provision of oxygen and nutrients for the host cells from the basal layer upwards provided us with the opportunity to develop a *C. parvum* culture medium that more closely approximates the intestinal lumen on the apical epithelial surface. *Cryptosporidium parvum* parasitises the lumen of the gut that has sub-micromolar oxygen tensions and the biochemistry of the parasite supports the presence of an anaerobic metabolism; the *C. parvum* genome reveals a lack of a Krebs cycle and oxidative phosphorylation and a striking increase in the number of amino acid and fatty acid transporters (Abrahamsen et al., 2004; Zhu, 2008). Addressing these nutritional and environmental requirements is necessary to developing a long-term culture system. To this end we developed a redox buffer with the aim of creating a low redox environment that would mimic that present in the gut (Circu and Aw, 2011). The redox buffer contained 20 mg mL⁻¹ each of glutathione, taurine, betaine and cysteine prepared in nitrogen gassed distilled water. This mix resulted in a higher oocyst production than the addition of a mix containing 20 mg mL⁻¹ each of DTT/cysteine or 20 mg mL⁻¹ each of mercaptoethanol/cysteine. Many parasites have specific lipid requirements that may not be provided by the addition of serum alone, and there is some evidence in the literature that *C. parvum* also has a selective lipid requirement (Mazumdar and Striepen, 2007; Bushkin et al., 2013) and to this end we focused on developing a lipid mix composed primarily of omega-3 lipids. The composition and final amount was determined by titration of individual components of the mix that produced the maximum number of oocysts. The lipid mix was composed of 1.5% deoxycholate, 6.7 mg mL⁻¹ oleic acid, 10 mg mL⁻¹ phosphocholine, 1.6 mg mL⁻¹ α-linolenic acid, 6.8 mg mL⁻¹ eicosapentaenoic acid, 2 mg mL⁻¹ docosahexaenoic acid, 18 mg mL⁻¹ cholesterol (dissolved in ethanol and mixed 1:1 with Tween 80). The extra capillary space of the cartridge (Fig. 1) was flushed with 50 mL of MEMSS (Upton et al., 1994) containing 1 μg mL⁻¹ resazurin (7-hydroxy-3H-phenoxazin-3-one 10 oxide) as a redox indicator, in place of phenol red, and containing the redox buffer and lipid mix as additives.

The cartridge was incubated for 2 h at 37 °C, during which time the resazurin indicator changed from a pink color (redox potential ≥ -51 mV) to colorless, indicating a redox potential of ≤ -110 mV. The redox potential was determined from a standard graph of the difference in the OD₅₇₀ nm to that at OD₆₀₀ nm versus the buffer redox potential in mV.

The cartridge was inoculated with 10⁶ *C. parvum* oocysts (Iowa isolate), and 3 mL samples removed daily by displacement using 3 mL of the MEMSS plus redox and lipid additives. Glucose consumption, pH, redox conditions and microscopic examination were recorded to determine the integrity of the host cell feeder layer and parasite development. The medium glucose levels present in the host cell medium exhibited a dampened oscillation over the first 10 days of the infection (Days 12–22, Fig. 2A) that may be the result of initial synchrony of disruption of the host cell monolayer caused by the infection. By day 23 the glucose consumption was approximately 50% of the added glucose in 24 h (Fig. 2B). The glucose concentration of the medium in the hollow fibers, providing nutrients to the host cells varied from 50 to 250 mg/dL, whereas the glucose concentration in the cartridge space (providing nutrients to the parasites) varied between 270 and 334 mg/dL over the duration of the study. The pH changed by -0.81 pH units over 48 h in the host cell medium, whereas it showed minor variation in the cartridge space (pH 6.99–7.09). These measurements indicate that there is a difference between the environments inside the cartridge (parasite environment) and that inside the hollow fibers (host cell nutrients). Samples inside the cartridge (5–10 mL) were removed weekly and examined under light microscopy (Fig. 3A) after dual staining using fluorescein-labeled polyclonal antibody for intracellular and motile stages (Sporo-Glo[®]; Fig. 3B), and FITC-labeled monoclonal antibody for oocysts (Crypt-a-Glo[®]; Fig. 3C). Parasites achieved a density of 1 ± 0.1 × 10⁸ oocysts per mL (Fig. 2C), and 8 ± 2 × 10⁷ intracellular motile stages per mL (Fig. 2D), in the hollow fiber culture system compared with 0.8 × 10⁶ per mL oocysts in 25 cm² flasks, and continued growing for >6 months (at time of submission) compared with 48 h when grown in 2D tissue culture.

3.2. Parasite enumeration by qRT-PCR

A second culture system was established to determine the effects of flow rate on parasite numbers and host cell maintenance (Fig. 4A). Parasite and sloughed host cell numbers were evaluated by determining the C_T of Cp18S rRNA and h18S rRNA for samples collected from the culture system. The h18S rRNA had minor variation over 15 weeks, and was therefore used to normalise the par-

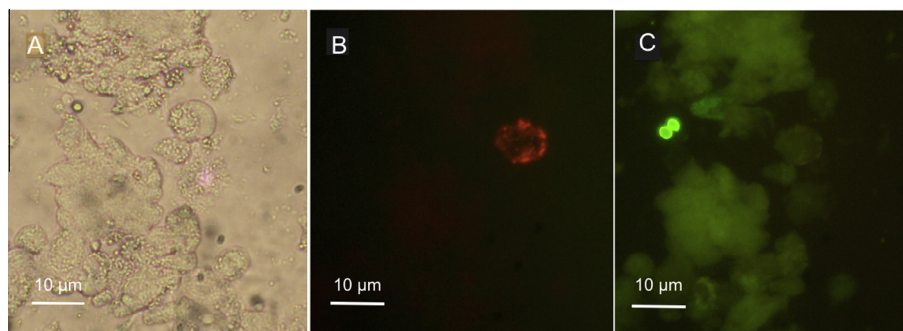


Fig. 3. Specificity of fluorescent antibody stages from the *Cryptosporidium parvum* culture. Samples collected from the culture were incubated at 26 °C with equal volumes of fluorescein-labeled polyclonal antibody to intracellular and motile stages of the parasite (Sporo-Glo[®], Waterborne Inc., New Orleans, LA, USA) and FITC-labeled monoclonal antibody to oocyst wall proteins (Crypt-a-Glo[®], Waterborne Inc.) for 30 min, washed three-times in PBS and examined microscopically. (A) Light microscopic image, ×400 magnification. (B) Fluorescence microscopic image for fluorescein-labeled antibody to intracellular and motile stages, excitation λ 535–550 nm, emission λ 580 nm. (C) Fluorescence microscopic image for FITC-labeled monoclonal antibody to oocysts, excitation λ 418–485 nm, emission λ 575 nm. Magnification 400-fold, antibodies for oocysts do not label intracellular or motile stages.

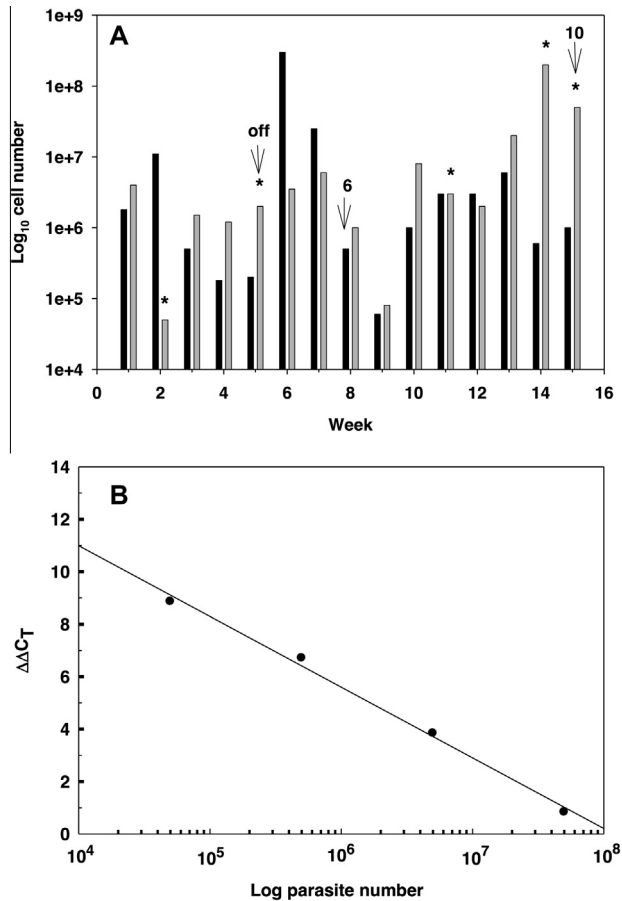


Fig. 4. Ratio of *Cryptosporidium parvum* to sloughed HCT-8 cells in the cartridge based on 18S rRNA. *Cryptosporidium parvum*, 18S-rRNA (Cp18S rRNA) and HCT-8, 18S rRNA (h18S rRNA) were quantitated in 5 ng of RNA purified samples removed from the culture system, using parasite specific primers as described in Section 2. (A) From the C_T of parasite and human 18S RNA, the ΔC_T was determined. Using a standard of log of parasite number (10^5 – 10^8) versus ΔC_T , the parasite yield is determined from the ΔC_T values obtained for samples removed from the column. Weeks 1–5 pump rate 10, weeks 5–6 pump off (\downarrow), weeks 6–8 pump rate 10 (\downarrow), weeks 8–15 pump rate 6 (\downarrow), week 15 pump rate 10. In weeks 6, 8 and 10, 10 mL of the column volume was removed. HCT-8 cells (6.2×10^6) were added to the culture system on days indicated (*). *Cryptosporidium parvum* (■), HCT-8 cells (■). (B) Standard oocyst number versus C_T curve used to calculate numbers of *C. parvum* oocysts from the culture system.

asite ΔC_T values. The ΔC_T (Cp18S rRNA – h18S rRNA) values were compared with a standard graph prepared using 10^5 – 10^8 oocysts, enabling determination of parasite numbers from the culture system (Fig. 4B). Using this method, parasite numbers varied from 10^5 to 5×10^8 per mL over 15 weeks (Fig. 4A). Parasite numbers showed a cyclical rhythm of 3–4 weeks. After 15 weeks the numbers of host cells in the sample collected increased, which may be indicative of a chronic infection resulting in significant damage to the host cell layer.

3.3. *Cryptosporidium parvum* oocysts infect immunosuppressed and immunodeficient mice

TCR- α -deficient mice infected with 10^4 oocysts (Fig. 5) harvested after 4 and 20 weeks in culture (Table 1); and dexamethasone immunosuppressed mice infected with 10^6 *C. parvum* oocysts harvested after 6 weeks in culture (Table 2) resulted in oocyst shedding in the feces at comparable numbers to the control Iowa isolate used to initiate the culture system. Mice infected with oocysts obtained from the 6th week of the culture system and the

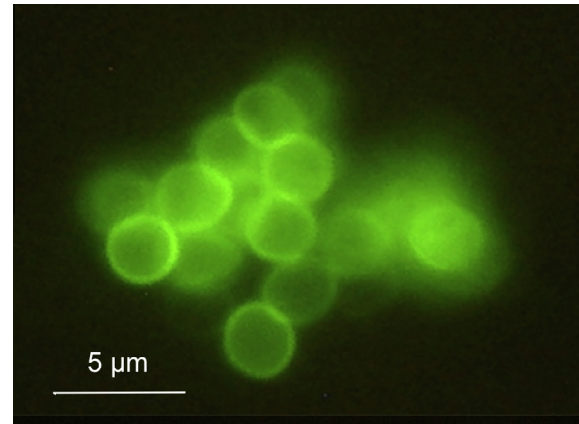


Fig. 5. FITC-labeled monoclonal antibody stained *Cryptosporidium parvum* oocysts from the culture. Oocysts were obtained from 5 mL of culture, washed with PBS and resuspended in 1 mL of buffer. An equal amount (50 μ L) of sample and FITC-labeled monoclonal antibody to oocyst cell wall protein and sample was incubated for 30 min. The reaction was stopped by centrifugation (14,000g) and washed three times before analyzing using excitation λ 418–485 nm, emission λ 575 nm.

Table 1

Immunocompromized mouse infection model. TCR- α -deficient mice were infected per os with 10^4 *Cryptosporidium parvum* oocysts from the 6 week and 20 week culture system, and compared with the parent Iowa isolate and uninfected controls. Feces were stored in potassium dichromate prior to microscopic examination after staining with a fluorescent monoclonal antibody to the oocyst cell wall (Crypt-a-Glo, Waterborne Inc, New Orleans, LA, USA).

Weeks since culture	Days p. i.	Sample		
		Uninfected control	Cultured oocysts	Iowa oocysts
4 weeks	4	0 \pm 0	1.5 + 0.7	1 + 1
	5	0 \pm 0	3 + 2	2.6 + 3
	6	0 + 0	13.3 + 8.6	7.7 + 8.9
20 weeks	12	0 \pm 0	9.6 + 8.2	15.8 + 6.3
	14	0 \pm 0	31.2 + 12.4	19.7 + 11.6
	17	0 \pm 0	29.8 + 19.7	42.3 + 26.4
	19	0 \pm 0	69.8 + 32.3	53.9 + 39.2
	21	0 \pm 0	159.2 + 41.8	87.5 + 51.4

Table 2

Immunosuppressed mouse infection model. Dexamethasone-treated CD-1 mice were infected per os with 10^6 *Cryptosporidium parvum* oocysts from the 6 week old culture system or the parent Iowa isolate. Feces were examined microscopically after staining by the modified Kinyoun acid fast method. The number of oocysts on a microscopic field of 13.5 mm² was counted.

Group	Mouse number	Days p.i.		
		13	14	17
Not treated	m1	0	0	0
	m2	0	0	0
	m3	0	0	0
	m4	0	0	0
	m5	0	0	0
Cultured oocysts	m1	0	1	8
	m2	7	5	151
	m3	3	0	0
	m4	15	96 ^a	NA
	m5	3	3	7
Iowa oocysts	m1	2	0	0
	m2	71	19	58 ^b
	m3	0	0	0
	m4	2	5	4
	m5	NA	NA	NA

^a The colon content was analyzed.

^b Fecal sample from 16 days post oocyst inoculation.

parent Iowa isolate demonstrated an average 17% weight loss compared with uninfected immunosuppressed control mice after day 10 (Fig. 6A). Post 10 days, oocyst shedding was detected in fecal samples from all of the mice infected with the culture system (Table 2). Oocyst shedding intensities were similar between the mice from both the culture-derived oocyst infection and the parent-derived oocyst infection. On day 14 the colon content was analyzed for mouse four from the culture-derived oocyst group (Table 2). Histological sections of the intestine (ileum) from mice 17 days p.i. demonstrated the presence of *C. parvum* life cycle stages in the terminal ilea and proximal colon (Fig. 6B).

3.4. *Cryptosporidium parvum* cultures have unchanged polyamine biosynthesis

Cryptosporidium parvum oocysts collected from the hollow fiber cartridge were purified by percoll gradients (Arrowood and Sterling, 1987) and the sporozoite stage obtained as described in Section 2. Homogenates of sporozoites were subjected to various biochemical analyses for comparison with data obtained using oocysts supplied from calf infections. We previously characterized the intracellular polyamine levels and their respective biosynthetic enzymes from *C. parvum* oocysts and sporozoites (Keithly et al., 1997; Morada et al., 2013). In many of the Apicomplexa the levels of putrescine and spermidine have been shown to increase dramatically during infection of the host cell (Niemand et al., 2012). These polycationic molecules are critical to parasite growth and development, and play a key role in the production of hypusine and therefore activation of eukaryotic initiation factor (eIF-5A), which is present in the parasite (Mittal et al., 2014). For this reason we evaluated parasites harvested from the cartridge for polyamine content and polyamine biosynthetic enzyme activity. The major polyamines putrescine, spermidine and spermine were determined by HPLC (Morada et al., 2013) to be 2.6 ± 0.9 , 41.7 ± 5.3 and 23.5 ± 2.1 pmol per 10^6 cells (\pm S.D. of triplicate results), respectively, which compared with 2.0, 47.8 and 20.0 pmol per 10^6 cells previously observed (Morada et al., 2013), and are within the S.D. of experimental variation. The activity of polyamine biosynthetic enzymes was also measured in parasites collected from the cartridge. SSAT, S-adenosyl-L-methionine decarboxylase (SAMdc, putrescine stimulated) and SAT had activities of 0.15 ± 0.05 , 0.009 ± 0.002 and 0.21 ± 0.04 nmol min⁻¹ (mg of protein)⁻¹, respectively (\pm S.D. of triplicate results), which compared favorably to published (Keithly et al., 1997) values of 0.12, 0.006 and 0.17 nmol min⁻¹ (mg of protein)⁻¹, respectively.

3.5. Electron microscopy of infected host cells grown on hollow fibers

The structure of the host cell layer was determined after 8 weeks of parasite growth. The cartridge case was opened and the hollow fibers cut into thin sections, fixed as described in Section 2, and examined by SEM (Fig. 7). After 8 weeks of growth on

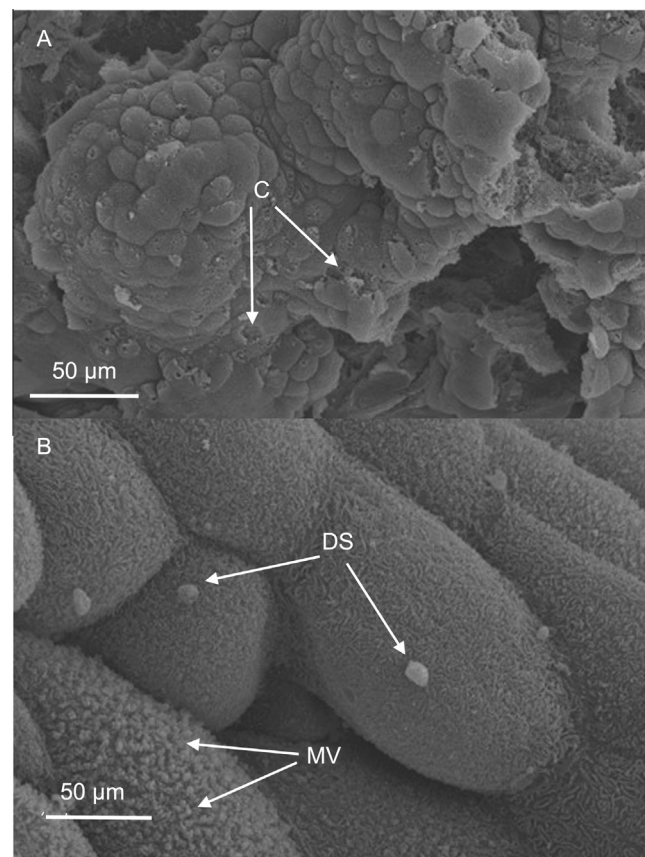


Fig. 7. Scanning Electron Microscopy of intestinal epithelial cells infected with *Cryptosporidium parvum*. After 8 weeks of growth, the cartridge was cut open and slices of thin sections of the hollow fibers examined by Scanning Electron Microscopy. The intestinal epithelial cells had differentiated into crypt-villus units with microvilli (MV) covering them. (A) Proximal end of the cartridge shows many craters (C) in the epithelial cell layer, typical of a *C. parvum* infection. (B) Distal end of the cartridge has less epithelial damage and developmental stages are visible as sacs covering the villi (DS).

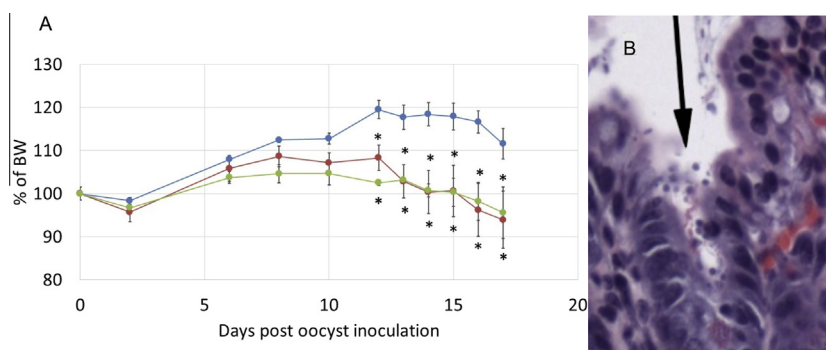


Fig. 6. Dexamethasone-immunosuppressed mouse infection model with *Cryptosporidium parvum* oocysts. Mice were weighed three times per week following dosing with *C. parvum* oocysts from the culture system and the parent Iowa isolate, and compared with uninfected controls. (A) Weights for five animals within each group were averaged and plotted as \pm S.E. (error bars). After 6–8 days, mice infected with *C. parvum* oocysts from the culture system or the parent Iowa isolate demonstrated significant weight loss compared with uninfected controls. Asterisks (*) indicate statistical differences ($P < 0.05$) between the untreated control group and groups infected with the culture or the parent Iowa oocysts. Untreated controls (—●—), cultured oocysts (—■—), Iowa parent isolate (—▲—). (B) H&E stains of gastrointestinal tissue from *C. parvum*-infected mice. Arrow indicates the presence of *C. parvum* stages.

hollow fibers, the intestinal epithelial cells had differentiated into crypt-villus units (Fig. 7). Developmental parasite stages were evident as sacs covering the epithelial cells, and at this early stage populated mainly the proximal end of the cartridge (Fig. 7A) where they were introduced. The epithelial layer has many craters and scars (Fig. 7A) characteristic of those previously observed in *Cryptosporidium* sp.-infected intestinal sections (Fayer, 2008). At the 8 week stage the distal end of the cartridge has a lower parasite load (Fig. 7B), which was mainly due to oocysts produced from the initial infection as the parasites move down the cartridge, mimicking the situation found in the gut of infected animals (Fayer, 2008). Oocysts collected from the cartridge were identified using a specific FITC labeled mouse anti *C. parvum* oocyst monoclonal antibody, and excysted (as described in Section 2) producing motile sporozoites. Oocysts (10^6) collected from the cartridge were used to infect a HCT-8 monolayer in 2D cultures using 75 cm² flasks containing 10 mL of MEM plus 10% horse serum. The medium was removed 3 h p.i. and replaced with fresh MEM plus 10% horse serum. After 24 h at 37 °C in a 5% CO₂ incubator, the flasks produced 2.6×10^6 oocysts compared with 3.2×10^6 oocysts ml⁻¹ in control flasks infected with 10^6 oocysts obtained from neonatal calves.

4. Discussion

Building on recent advances in the genomic, biochemical and in vitro culture methods of *Cryptosporidium* research, we have developed a method for the long-term in vitro culture of *C. parvum* using hollow fiber technology. In developing the method, we concentrated on a design that would permit control of two separate environments (biphasic), permitting an aerobic nutrient supply to the host cells, while also allowing a separate anaerobic nutrient rich medium to be established for the parasite environment. The ability to generate the intestinal redox conditions is a critical factor in the success of the method. It has been determined that under physiological conditions the *Eh* for the oxidised/reduced (GSH/GSSG) glutathione couple is between –260 and –200 mV (Kemp et al., 2008). Intestinal epithelial cells have a highly reduced cytosolic glutathione pool (*Eh* for GSH/GSSG of –260 mV) whereas the inter-membranous space is slightly more oxidised (*Eh* of –255 mV) and the endoplasmic reticulum matrix is highly oxidised (*Eh* –170 to –185 mV), ensuring correct folding of nascent proteins (Circu and Aw, 2011). The luminal glutathione pool is efficiently taken up by the intestinal epithelial cells and is important for normal growth and development of these cells. It has been shown that changes in the redox potential correlate with intestinal cell phenotypes. A reducing redox environment (*Eh* –260 mV to –240 mV) favors proliferation, whereas an oxidised one (*Eh* –220 mV to –200 mV) favors differentiation and under highly oxidised conditions growth arrest occurs (*Eh* –170 mV), which is followed by necrosis or apoptosis at an *Eh* –150 mV (Jonas et al., 2002). The luminal cysteine pool is also a key player in redox control as a significant proportion of the extracellular glutathione pool is hydrolysed to cysteine (Kemp et al., 2008). Redox control of extracellular surface proteins by luminal cysteine is believed to regulate signaling processes at the apical plasma membrane (Jonas et al., 2002). Glutamine was included as an additive because it has been shown that this amino acid contributed to a more reduced extracellular cysteine pool, resulting in enhanced CaCo-2 cell growth by activation of redox signaling at the plasma membrane (Jonas et al., 2002). In addition glutathione is essential for the intestinal elimination of luminal peroxidised lipids (Circu and Aw, 2011), which if not removed would deter parasite colonisation of the epithelial cells. In this regard *C. parvum* sporozoites infect host cells in the crypts of the villi and develop into meronts as

the epithelial cell migrates to the apical tip where the merozoites escape from the parasitophorous vesicle.

Biochemical and genomic data agree that *C. parvum* lacks a typical mitochondrion, oxidative phosphorylation pathway and a Krebs cycle, relying upon glycolysis and fatty acid oxidation for energy production (Mazumdar and Striepen, 2007; Zhu, 2008). The low redox environment of the media employed in this study would therefore favor the growth and development of a parasite with a fermentative metabolism.

In support of this hypothesis, the yield of parasites obtained from the culture system was significantly improved by including a lipid supplement which included the omega-3 fatty acids, α -linolenic acid, eicosapentaenoic acid and docosahexaenoic acid. Recently it has been shown that *C. parvum* oocyst walls are acid-fast and contain a complex set of triglycerides rich in polyhydroxy and long fatty acyl chains that may be synthesized by a polyketide synthase (Zhu et al., 2010; Bushkin et al., 2013). This wax-like rigid bilayer is impermeable to disinfectants and environmental stress, and is essential for continued propagation of the parasite. *Cryptosporidium parvum* lacks fatty acid synthase II biosynthetic machinery, suggesting they are dependent upon fatty acid salvage from the host (Zhu et al., 2010). However the parasite does possess a fatty acid synthase I complex that resembles a polyketide synthase that is proposed to act as a fatty acyl elongase and is responsible for the production of the long acyl chain fatty acids required for the formation of the oocyst cell wall (Mazumdar and Striepen, 2007). Hence it is likely that the medium chain fatty acids added to the extra capillary space favor formation of the thick cell wall oocyst stage and propagate the infection. Thick walled oocysts are shed in the feces of infected individuals and serve to transmit the infection; once ingested these thick walled oocysts pass through the stomach and produce motile sporozoites in the small intestine that infect the host epithelial cells, resulting in an asexual cycle that produces Type I meronts which reinfect epithelial cells; the problem with current culture conditions is that the merozoites produced at this stage fail to enter the sexual cycle, producing Type II meronts that ultimately produce zygotes which transform into thin walled oocysts, resulting in auto-infection or thick walled oocysts that are excreted and are responsible for disease transmission. That the oocysts from the culture system undergo a complete life cycle is demonstrated using the well described and validated mouse model that employs either the dexamethasone immunosuppressed mice, or the genetically modified TCR- α -immunocompromised mouse model.

Hollow fiber technology has successfully been used to produce a constant supply of large numbers of *Plasmodium falciparum* for pharmacokinetic analysis of potential chemotherapeutic compounds (Bakshi et al., 2013) which mimicked the dynamic fluctuations of the drug in vivo, providing clinically relevant data that could be used to select antimalarial lead compounds based upon total exposure, peak concentration or time above the minimum inhibitory concentration, providing preclinical pharmacokinetic data in the absence of animal models. We are currently adapting our method to perform a similar pharmacokinetic function that will allow us to obtain critical information needed for the development of chemotherapeutic agents to treat disease caused by this parasite.

Hollow fiber technology provides several unique features: (i) a large surface area for metabolite and gas exchange, which are needed for efficient growth of host cells; (ii) the creation of a biphasic medium providing an oxygen rich nutrient supply to the basal layer of the host cells, while permitting the provision of an anaerobic nutrient rich supply to the apical side mimicking the gut; (iii) the ability to obtain high numbers of in vitro cultured *C. parvum* oocysts for biochemical and molecular studies; (iv) study of the host-parasite relationship in a long-term in vitro infection;

(v) the ability to obtain in vitro preclinical pharmacokinetic data, providing a unique method for drug selection; and (vi) this method can also be used for analysis and preparative isolation of *Cryptosporidium* growth factors.

Acknowledgements

This paper is dedicated to the memory of Seymour H. Hutner (10/31/1911–6/1/2003) whose inspiration lives on. Thank you to Dr. Guan Zhu (Texas A & M University, TX, USA) for helpful discussions concerning qRT-PCR analysis of parasites from the culture system. Thanks to Elena Mejia and Donna Sarno for providing excellent technical assistance and Dr. Cyrus Bacchi for helpful discussions. The research was supported in part by grants from the Bill and Melinda Gates Foundation, USA, OPP1117675 (NY); The National Institutes of Health, National Institute of Allergy and Infectious Diseases, USA AI095094 (LW); and Cancer Center, USA grant NCI P30CA013330 (LW).

References

- Abrahamsen, M.S., Templeton, T.J., Enomoto, S., Abrahante, J.E., Zhu, G., Lancto, C.A., Deng, M., Liu, C., Widmer, G., Tzipori, S., Buck, G.A., Xu, P., Bankier, A.T., Dear, P. H., Konfortov, B.A., Spriggs, H.F., Iyer, L., Anantharaman, V., Aravind, L., Kapur, V., 2004. Complete genome sequence of the apicomplexan, *Cryptosporidium parvum*. *Science* 304, 441–445.
- Abubakar, I., Aliyu, S.H., Arumugam, C., Usman, N.K., Hunter, P.R., 2007. Treatment of cryptosporidiosis in immune-compromised individuals: systematic review and meta-analysis. *Br. J. Clin. Pharmacol.* 63, 387–393.
- Alcantara Warren, C., Destura, R.V., Sevilleja, J.E., Barroso, L.F., Carvalho, H., Barrett, L.J., O'Brien, A.D., Guerrant, R.L., 2008. Detection of epithelial cell injury and quantification of infection in the HCT8 organoid model of cryptosporidiosis. *J. Infect. Dis.* 198, 143–149.
- Arrowood, M.J., 2008. *In vitro* cultivation. In: Fayer, R., Xiao, L. (Eds.), *Cryptosporidium* and *Cryptosporidiosis*, second ed. CRC Press, Boca Raton, USA, pp. 499–525.
- Arrowood, M.J., Sterling, C.R., 1987. Isolation of *Cryptosporidium* oocysts and sporozoites using discontinuous sucrose and isopycnic percoll gradients. *J. Parasitol.* 74, 314–319.
- Bakshi, R.P., Nenorlas, E., Tripathi, A.K., Sullivan, D.J., Shapiro, T.A., 2013. Model system to define pharmacokinetic requirements for antimalarial drug efficacy. *Sci. Transl. Med.* 5 (205), 205ra135. <http://dx.doi.org/10.1126/scitranslmed.3006684>.
- Banwat, E.B., Egah, D.Z., Onile, B.A., Angyo, I.A., Audu, E.S., 2003. Prevalence of *Cryptosporidium* infection among undernourished children in Jos, Central Nigeria. *Niger. Postgrad. Med. J.* 10, 84–87.
- Bushkin, G.G., Motari, E., Carpentieri, A., Dubey, J.P., Costello, E.E., Robbins, P.W., Samuelson, J., 2013. Evidence for a structural role for acid-fast lipids in oocyst walls of *Cryptosporidium*, *Toxoplasma* and *Eimeria*. *MBio* 4, e00387–e00413. <http://dx.doi.org/10.1128/mBio.00387-13>.
- Carvalho, H.M., Teel, L.D., Goping, G., O'Brien, A.D., 2005. A three-dimensional tissue culture model for the study of attach and efface lesion formation by enteropathogenic and enterohaemorrhagic *Escherichia coli*. *Cell. Microbiol.* 7, 1771–1781.
- Cai, X., Woods, K.M., Upton, S.J., Zhu, G., 2005. Application of quantitative real-time reverse transcription-PCR in assessing drug efficacy against the intracellular pathogen *Cryptosporidium parvum* in vitro. *Antimic. Ag. Chemother.* 49, 4437–4442.
- Castellanos-Gonzalez, A., Cabada, M.M., Nichols, J., Gomez, G., White, A.C., 2013. Human primary intestinal epithelial cells as an improved in vitro model for *Cryptosporidium parvum* infection. *Infect. Immun.* 81, 1996–2001.
- Checkley, W., White, A.C., Jaganath, D., Arrowood, M.J., Chalmers, R.M., Chen, X., Fayer, R., Griffiths, J.K., Guerrant, R.L., Hedstrom, L., Huston, C.D., Kotloff, K.L., Kang, G., Mead, J.R., Miller, M., Petri Jr., W.A., Priest, J.W., Roos, D.S., Striepen, B., Thompson, R.C., Ward, H.D., Van Voorhis, W.A., Xiao, L., Zhu, G., Houpt, E.R., 2014. A review of the global burden, novel diagnostics, therapeutics, and vaccine targets for *Cryptosporidium*. *Lancet Infect. Dis.* 15 (1), 85–94.
- Circu, M.L., Aw, T.Y., 2011. Redox biology of the intestine. *Free Radical Res.* 45, 1245–1266.
- Fayer, R., 2008. General biology. In: Fayer, R., Xiao, L. (Eds.), *Cryptosporidium* and *Cryptosporidiosis*, second ed. CRC Press, Boca Raton, USA, pp. 1–42.
- Hamed, Y., Safa, O., Haidari, M., 2005. *Cryptosporidium* infection in diarrheic children in southeastern Iran. *Pediatr. Infect. Dis. J.* 24, 86–88.
- Hieinz, E., Lithgow, T., 2013. Back to basics: revealing secondary reduction of the mitochondrial protein import pathway in diverse intracellular parasites. *Biochim. Biophys. Acta* 1833, 295–303.
- Jonas, C.R., Ziegler, T.R., Gu, L.H., Jones, D.P., 2002. Extracellular thiol/disulfide redox state affects proliferation rate in a human colon carcinoma (Caco2) cell line. *Free Radical Biol. Med.* 33, 1499–1506.
- Keithly, J.S., Zhu, G., Upton, S.J., Woods, K.M., Martinez, M.P., Yarlett, N., 1997. Polyamine biosynthesis in *Cryptosporidium parvum* and its implications for chemotherapy. *Mol. Biochem. Parasitol.* 88, 35–42.
- Kemp, M., Go, Y.M., Jones, D.P., 2008. Non-equilibrium thermodynamics of thiol/disulfide redox systems: a perspective on redox systems biology. *Free Radical Biol. Med.* 44, 921–937.
- Kotloff, K.L., Nataro, J.P., Blackwelder, W.C., Nasrin, D., Faraq, T.H., Panchalingam, S., Wu, Y., Sow, S.O., Sur, D., Breiman, R.F., Faruque, A.S., Zaidi, A.K., Saha, D., Alonso, P.L., Tamboura, B., Sanogo, D., Onwuchekwa, U., Manna, B., Ramamurthy, T., Kanungo, S., Ochleng, J.B., Omoro, R., Oundo, J.O., Hossain, A., Das, S.K., Ahmed, S., Qureshi, S., Quadri, F., Adegbola, R.A., Antonio, M., Hossain, M.J., Akinsola, A., Mandomando, I., Nhamposha, T., Acacio, S., Biswas, K., O'Reilly, C.E., Mintz, E.D., Berkeley, L.Y., Muhsen, K., Sommerfeit, H., Robins-Browne, R.M., Levine, M.M., 2013. Burden and etiology of diarrheal disease in infants and young children in developing countries (the Global Enteric Multicenter Study, GEMS): a prospective, case-control study. *Lancet* 382, 209–222.
- Liu, L., Johnson, H.L., Cousens, S., Perin, J., Scott, S., Lawn, J.E., Rudan, I., Campbell, H., Cibulskis, R., Li, M., Mathers, C., Black, R.E., 2012. Child Health Epidemiology Reference Group of WHO and UNICEF, 2012. Global, regional, and national causes of child mortality: an updated systematic analysis for 2010 with time trends since 2000. *Lancet* 379, 2151–2161.
- Ma, P., Soave, R., 1983. Three-step stool examination for cryptosporidiosis in 10 homosexual men with protracted watery diarrhea. *J. Infect. Dis.* 147, 824–828.
- Mathur, M.K., Verma, A.K., Makwana, G.E., Sinha, M., 2013. Study of opportunistic parasitic infections in human immunodeficiency virus/acquired immunodeficiency syndrome patients. *J. Global Infect. Dis.* 5, 164–167.
- Mazumdar, J., Striepen, B., 2007. Make it or take it: fatty acid metabolism of apicomplexan parasites. *Eukaryotic Cell* 6, 1727–1735.
- Meloni, B.P., Thompson, R.C., 1996. Simplified methods for obtaining purified oocysts from mice and for growing *Cryptosporidium parvum* in vitro. *J. Parasitol.* 82, 757–762.
- Mittal, N., Morada, M., Tripathi, P., Gowri, V.S., Mandal, S., Quirch, A., Park, M.H., Yarlett, N., Madhubala, R., 2014. *Cryptosporidium parvum* has an active hypusine biosynthesis pathway. *Mol. Biochem. Parasitol.* 195, 14–22.
- Mølbaek, K., Højlyng, N., Ingholt, L., Da Silva, A.P., Jepsen, S., Aaby, P., 2013. An epidemic outbreak of cryptosporidiosis: a prospective community study from Guinea-Bissau. *Pediatr. Infect. Dis. J.* 9, 566–570.
- Molloy, S.F., Tanner, C.J., Kirwan, P., Asaolu, S.O., Smith, H.V., Nichols, R.A., Connelly, L., Holland, C.V., 2011. Sporadic *Cryptosporidium* infection in Nigerian children: risk factors with species identification. *Epidemiol. Infect.* 239, 946–954.
- Morada, M., Pendyala, L., Wu, G., Merali, S., Yarlett, N., 2013. *Cryptosporidium parvum* induces an endoplasmic stress response in the intestinal adenocarcinoma HCT-8 cell line. *J. Biol. Chem.* 288, 30356–30364.
- Niemand, J., Louw, A.L., Birkholtz, L., Kirk, K., 2012. Polyamine uptake by the intraerythrocytic malaria parasite, *Plasmodium falciparum*. *Int. J. Parasitol.* 42, 921–929.
- Sifuentes, L.Y., DiGiovanni, G.D., 2007. Aged HCT-8 cell monolayers support *Cryptosporidium parvum* infection. *Appl. Environ. Microbiol.* 73, 7548–7551.
- Striepen, B., 2013. Parasitic infections: time to tackle cryptosporidiosis. *Nature* 503, 189–191.
- Upton, S.J., Tilley, M., Brillhart, D.B., 1994. Comparative development of *Cryptosporidium parvum* (Apicomplexa) in 11 continuous host cell lines. *FEMS Microbiol. Lett.* 118, 233–236.
- Varughese, E.A., Bennett-Stamper, C.L., Wymer, L.J., Yadav, J.S., 2014. A new in vitro model using small intestinal epithelial cells to enhance infection of *Cryptosporidium parvum*. *J. Microbiol. Met.* 106, 47–54.
- Xiao, L., 2010. Molecular epidemiology of cryptosporidiosis: an update. *Exp. Parasitol.* 124, 80–89.
- Yichou, M., Duarte, T.T., De Chatterjee, A., Mendez, T.L., Aguilera, K.Y., Roy, D., Roychowdhury, S., Aley, S.B., Das, S., 2011. Lipid metabolism in *Giardia*: a post-genomic perspective. *Parasitology* 138, 267–278.
- Zhu, G., 2008. Biochemistry. In: Fayer, R., Xiao, L. (Eds.), *Cryptosporidium* and *Cryptosporidiosis*, second ed. CRC Press, Boca Raton, USA, pp. 57–77.
- Zhu, G., Shi, X., Cai, X., 2010. The reductase domain in a type I fatty acid synthase from the apicomplexan *Cryptosporidium parvum*: restricted substrate preferences towards very long chain fatty acyl thioesters. *BMC Biochem.* 11, 46. <http://dx.doi.org/10.1186/1471-2091-11-46>.